

Numerical viscosity in hydrodynamics simulations in general relativity

P. Cerdá-Durán

Max-Planck-Institut für Astrophysik, Karl-Schwarzschild-st. 1, D-85741
Garching bei München, Germany

E-mail: cerda@mpa-garching.mpg.de

Abstract. We present an alternative method to estimate the numerical viscosity in simulations of astrophysical objects, which is based in the damping of fluid oscillations. We apply the method to general relativistic hydrodynamic simulations using spherical coordinates. We perform 1D-spherical and 2D-axisymmetric simulations of radial oscillations in spherical systems. We calibrate first the method with simulations with physical bulk viscosity and study the differences between several numerical schemes. We apply the method to radial oscillations of neutron stars and we conclude that the main source of numerical viscosity in this case is the surface of the star. We expect that this method could be useful to compute the resolution requirements and limitations of the numerical simulations in different astrophysical scenarios in the future.

PACS numbers: 95.30.Lz, 95.30.Sf, 97.60.Bw

Submitted to: *Class. Quantum Grav.*

1. Introduction

There is a number of scenarios in theoretical astrophysics which need to be modelled by means of numerical simulations. The complexity found in these scenarios does not allow for a simple analytical study to explain the observations. In a subset of these scenarios the effects of general relativity are important and a Newtonian description of the system is not sufficient. Some examples of stellar size scenarios of this kind are: i) the collapse of massive stellar cores to form a neutron star, which eventually can lead to a supernova explosion, ii) for more massive stars, the collapse to a black hole and possibly an accretion disk, which can power a long-duration gamma-ray burst (GRB) according to the collapsar scenario (Woosley 1993) and could be related to the subclass of broad-lined type Ic supernovae (Modjaz *et al* 2008), and iii) the cooling of a rapidly rotating hot proto-neutron star (PNS) to form a magnetar (Thomson & Duncan 1993). All three previous examples have in common that are quasi-spherical scenarios. Therefore it is natural to model them in numerical simulations using spherical polar coordinates.

Those scenarios have some common points. The three scenarios include multi-scale physics in which a broad range of length and time scales play an important role. In the supernova core collapse case the length scales to cover range from

the size of the iron core (~ 1000 km) to the size of the PNS (~ 10 km). The smaller length-scale process dominating the dynamics ranges from ~ 1 km in the case of convectively unstable PNS formed after the collapse of the most common slow rotating progenitors (Müller & Janka 1997), to 1 cm - 1 m if the magneto-rotational instability develops in the collapse of fast rotating progenitors (Cerdá-Durán *et al* 2007). Furthermore the mechanism for the explosion requires an appropriate modeling of the neutrino transport. The energy deposited by neutrinos behind the shock and the standing accretion-shock instability (SASI) probably are crucial for a successful explosion (Marek & Janka 2009). In the collapsar scenario strong rotation is necessary for the formation of a GRB. It allows the generation of an accretion disk around the formed black hole with a low-density funnel along the rotation axis. The relativistic jet which is responsible for the GRB is powered either by MHD processes or by the energy deposition of annihilating neutrinos around the axis (see e.g. MacFadyen *et al* 2001). In the first case, magneto-rotational instabilities and dynamo processes are most probably responsible for the amplification of the magnetic field during the collapse. The case of dynamo processes in rapidly rotating PNS resembles the modeling of the sun. The cooling time-scale is of the order of seconds while the rotation period which drives the dynamo processes can be as low as 1 ms reaching magnetic Reynolds number of $\sim 10^{17}$ (Thompson & Duncan 1993). The numerical modeling of all scenarios described above require very high resolution to resolve the MRI and the turbulence amplifying the magnetic field, full three-dimensional simulations to correctly capture the growth and saturation of the different types of instabilities (MRI, SASI, global MHD instabilities), and a time evolution much larger than the characteristic dynamical timescale of the system. Therefore the numerical methods intended to solve this problem should be as less dissipative as possible in order to guarantee that the numerical dissipation is smaller than the expected physical one or, in cases where the computational requirements do not allow this, the global properties of the system show convergence with increasing grid resolution. The numerical dissipation could be a serious limitation for the successful modeling of objects mentioned above. It is hence important to have the appropriate scaling with the resolution, which is a necessary property to have scalable numerical codes which can run efficiently in massive parallel computers.

Most of the numerical codes performing simulations of these scenarios use Eulerian grids, explicit numerical schemes, and a mesh adapted to the problem, mostly with grids in spherical polar coordinates. Eulerian grid-based codes are better suited for these scenarios than Lagrangian methods (e.g. smoothed particle hydrodynamics) because they allow to use finite-volume conservative schemes. Eulerian methods allow for the correct treatment of arbitrarily high discontinuities and shocks in general relativity (Ibañez *et al* 2000, Dimmelmeier *et al* 2002, Duez *et al* 2003, Shibata 2007, Baiotti *et al* 2007), even with magnetic fields (Gammie *et al* 2003, Komissarov *et al* 2005, Anninos *et al* 2005, Antón *et al* 2006). Explicit methods are better suited for multidimensional simulations since they are computationally less expensive and easier to parallelize, although they have time-step limitations given by the CFL condition (Courant *et al* 1928, 1967). Spherical polar coordinates have several properties which make them appropriate to model the objects described above: i) are well adapted for quasi-spherical objects, ii) allow for accurate conservation of angular momentum, which is not true, in general, for Eulerian grids (see e.g. Zink *et al* 2008 and Fragile *et al* 2009), iii) axisymmetry and spherical symmetry can be easily enforced, and iv) large radial domains can be covered using non equally spaced radial grids. These

numerical methods have been successfully applied in 1D (spherical symmetry) and 2D (axisymmetry) simulations. However the extension to 3D in spherical coordinates suffers from severe time-step restrictions which render simulations unaffordable unless a special treatment of the central and polar regions is used (see. e.g Mller & Janka 1997)

Numerical dissipation effects are present in simulations using Eulerian grids due to the discretization of the equations that are solved. There are several methods to quantify the amount of numerical dissipation of a code based on the measure of the energy losses of the system. This has been standard practice since the first studies of hydrodynamic turbulence (e.g. Herring *et al* 1974) due to the necessity of resolving the physical dissipation scales. There are also studies of the decay of waves in hydrodynamics (Porter *et al* 1994) and MHD simulations (e.g. Simon & Hawley 2009). More recently the numerical dissipation has been estimated measuring the angular momentum transport by MHD turbulence (Fromang & Papaloizou 2007, Simon *et al* 2009). All these methods allow for a simplified numerical setup in where the local dissipation properties of the numerical algorithms can accurately be estimated. We propose an alternative approach to measure the numerical dissipation that is suitable for global simulations of relativistic stars close to the equilibrium.

The aim of this paper is to study the effects of numerical viscosity in simulations with spherical coordinates and study the influence of the grid resolution and the numerical scheme. In section 2 we describe the hydrodynamics equations including physical bulk viscosity in general relativity (GR), in section 3 we present a method to estimate numerical dissipation effects in a simplified test case. We apply this method in section 4 to estimate the numerical viscosity of oscillating neutron stars. We finish the paper in section 5 discussing the implications of our numerical results. If is not explicitly mentioned, we use units in which $c = G = 1$. Greek indices run from 0 to 3 and Latin indices from 1 to 3.

2. GR hydrodynamics with bulk viscosity

We use the 3+1 decomposition of the spacetime in which the metric reads

$$ds^2 = g_{\mu\nu} dx^\mu dx^\nu = -\alpha^2 dt^2 + \gamma_{ij} (dx^i + \beta^i dt)(dx^j + \beta^j dt), \quad (1)$$

where α , β^i and γ^{ij} are the lapse function, the shift vector and the spatial 3-metric respectively. In addition we consider the conformally flat condition (CFC) approximation (Isenberg 2008, Wilson *et al* 1996) for the 3-metric $\gamma_{ij} = \phi^4 f_{ij}$, where ϕ is the conformal factor and f_{ij} the flat 3-metric in spherical coordinates. This approximation uses the maximal slicing condition and quasi-isotropic coordinates as gauge conditions. Under this approximation the resulting system consist in a hierarchy of elliptic equations (Cordero-Carrión *et al* 2009).

To be able to study numerical dissipation effects we need a physical counterpart to calibrate our results. We use for this purpose the bulk viscosity of the fluid. The energy momentum tensor of a fluid with bulk viscosity (Ehlers 1961) is

$$T^{\mu\nu} = \rho(1 + \epsilon)u^\mu u^\nu + (P - \zeta\Theta)h^{\mu\nu}, \quad (2)$$

where ρ is the rest-mass density, ϵ is the specific internal energy, u^μ is the 4-velocity of the fluid, P is the pressure, ζ is the bulk viscosity, $\Theta \equiv u^\mu_{;\mu}$ is the expansion of the fluid and $h^{\mu\nu} \equiv g^{\mu\nu} + u^\mu u^\nu$. The bulk viscosity appears as an isotropic term in the energy-momentum tensor in a very similar way to the pressure. Therefore we can

define a modified pressure $\hat{P} \equiv P - \zeta\Theta$ such that the energy-momentum tensor has the same form as a perfect fluid

$$T^{\mu\nu} = \rho \hat{h} u^\mu u^\nu + \hat{P} g^{\mu\nu}, \quad (3)$$

where $\hat{h} \equiv h - \zeta\Theta/\rho$, being $h \equiv 1 + \epsilon + P/\rho$ the relativistic specific enthalpy. Using this form of the energy-momentum tensor is easy to modify an existing hydrodynamics code to include bulk viscosity, specially if the next assumptions are taken into account: i) we approximate the expansion assuming a post-Newtonian expansion and small perturbations,

$$\Theta = \nabla \cdot \mathbf{u} + \mathcal{O}(c^{-2}) + \mathcal{O}(v^2), \quad (4)$$

where $\mathcal{O}(c^{-2})$ corresponds to first post-Newtonian corrections. All the simulations that we run with physical bulk viscosity in this work belong to this regimen. ii) The bulk viscosity coefficient ζ is sufficiently small, such that $\hat{P} > 0$. And iii) we neglect the contribution of the bulk viscosity in the computation of the sound speed needed for our numerical scheme.

The hydrodynamics equations with bulk viscosity can be cast as a system of conservation laws (cf. Ibañez *et al* 2000)

$$\partial_t (\sqrt{\gamma} D) + \partial_i [\sqrt{\gamma} D v^{*i}] = 0, \quad (5)$$

$$\partial_t (\sqrt{\gamma} S_j) + \partial_i [\sqrt{\gamma} (S_j v^{*i} + \delta_j^i \alpha \hat{P})] = \frac{1}{2} \alpha \sqrt{\gamma} T^{\mu\nu} \partial_j g_{\mu\nu}, \quad (6)$$

$$\partial_t (\sqrt{\gamma} \tau) + \partial_i [\sqrt{\gamma} (\tau v^{*i} + \alpha \hat{P} v^i)] = \alpha^2 \sqrt{\gamma} (T^{\mu 0} \partial_\mu (\ln \alpha) - T^{\mu\nu} \Gamma_{\mu\nu}^0) \quad (7)$$

where $D \equiv \rho W$, $S_j \equiv \rho \hat{h} W^2 v_j$, $\tau \equiv \rho \hat{h} W^2 - \hat{P} - D$ are the conserved variables, $v^{*i} \equiv dx^i/dt$ is the coordinate 3-velocity, $v^i = (v^{*i} - \beta^i)/\alpha$ is the 3-velocity as measured by an Eulerian observer, and $W = 1/\sqrt{1 - \gamma_{ij} v^i v^j}$ the Lorentz factor. In the non-relativistic limit the equations for a classical viscous fluid can be recovered (Landau & Lifschitz 1987) which for constant ζ result in the Navier-Stokes equations.

We solve the coupled system of CFC spacetime evolution and GR hydrodynamics equations using the numerical code COCONUT (Dimmelmeier *et al* 2002, 2005). The numerical code uses standard high-resolution shock-capturing schemes for the hydrodynamics evolution in spherical polar coordinates, and spectral methods for the spacetime evolution.

3. Estimating numerical viscosity

To estimate the numerical viscosity of our code we have designed a simple spherical test. We consider a spherical fluid system of radius R and constant density in a static Minkowski spacetime. This system allow for discrete modes of radial oscillations (see appendix A). Since the eigenfunctions of the modes are known it is possible to excite very accurately single modes of the system and follow their evolution. We evolve the system using a polytropic equation of state, therefore, since the system is adiabatic, there are no possible energy losses and the oscillations should keep constant amplitude as long as non-linear effects does not appear. Hence, any damping observed in the numerical simulation has to be caused by numerical dissipation effects.

We have chosen a system with $R = 1$ and initial density $\rho_0 = 1$. The equation of state is a polytrope of the form $P = K \rho^\Gamma$ with $\Gamma = 4/3$ and $K = 1/3 \times 10^{-3}$. We use a perturbation $A(r)$ (see appendix A) of the velocity with an amplitude of

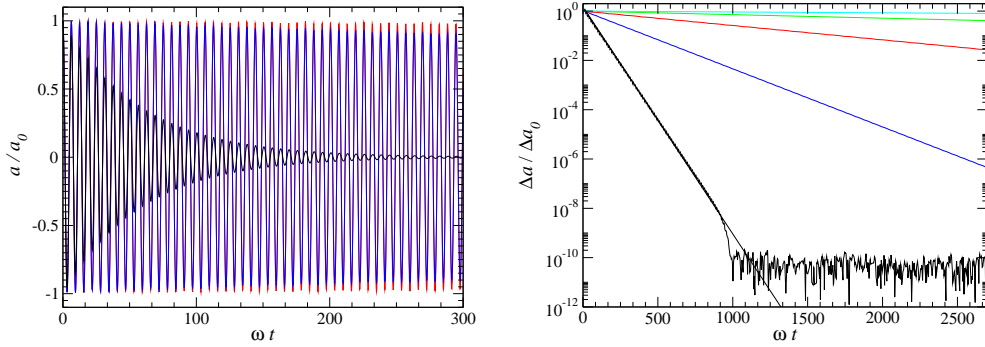


Figure 1. Time evolution of the first oscillation mode in the spherical test system. All evolutions shown are computed using the Marquina flux formula. Left panel shows the evolution of the perturbation a normalized to its initial value a_0 for a radial resolution $n_r = 80$ and different reconstruction procedures: constant (black line), minmod (blue line) and MC (red line). The right panel shows the evolution of the amplitude of the perturbation Δa normalized to its initial value Δa_0 using minmod reconstruction and different resolutions: 10 (black), 20 (blue), 40 (red), 80 (green) and 160 (cyan). We also plot the fit of the lowest resolution simulation to an exponential decay (black line).

$v'_0 = 10^{-5}$ corresponding to the lowest frequency mode, $\omega = 0.094$. This amplitude is sufficiently small for the oscillations to be considered linear. We have used second order Runge-Kutta method for the time evolution in all cases and two different flux formulae, Marquina (Donat et al 1998) and HLL (Harten & van Leer 1983). We have computed all models using different reconstruction techniques (constant and linear with minmod or MC slope limiters) and different resolutions ($n_r = 10, 20, 40, 80$ and 160). We have also computed the models without physical bulk viscosity ($\zeta = 0$) and with non-zero values ($\zeta = 10^{-4}, 10^{-5}$ and 10^{-6}). We have evolved the system for $2700 \omega^{-1}$. To follow the evolution of the oscillations we computed the quantity

$$a(t) = \int dx^3 A(r) v^r(r, t). \quad (8)$$

Left panel of figure 1 shows the time evolution of a/a_0 for different reconstruction procedures, a_0 being the initial value of a . The oscillation frequency coincides with the predicted by the linear analysis within 0.1% for $n_r = 80$. It can be seen that the order of the reconstruction has a strong influence in the numerical damping of the system, being much stronger for first order reconstruction (constant) than for second order (minmod or MC). In order to quantify this effect we estimate the damping time for each simulation as it is described next. In every case, we first compute the amplitude of a as the difference between two consecutive oscillations, Δa . In the right panel of figure 1 we plot the evolution of the amplitude for the minmod reconstruction case for five different resolutions. For very low resolution, the amplitude of the perturbation falls below the round-off error of the code within the duration of the simulation and it saturates. We fit next the the amplitude of the oscillations to an exponential decay $\Delta a(t) = \Delta a(0) e^{-2t/\tau}$ for each model. This procedure allow us to compute the value of the damping time of the amplitude, $\tau/2$. Since the energy of the perturbations scales quadratically with the velocity, the damping time of the energy is τ . Finally,

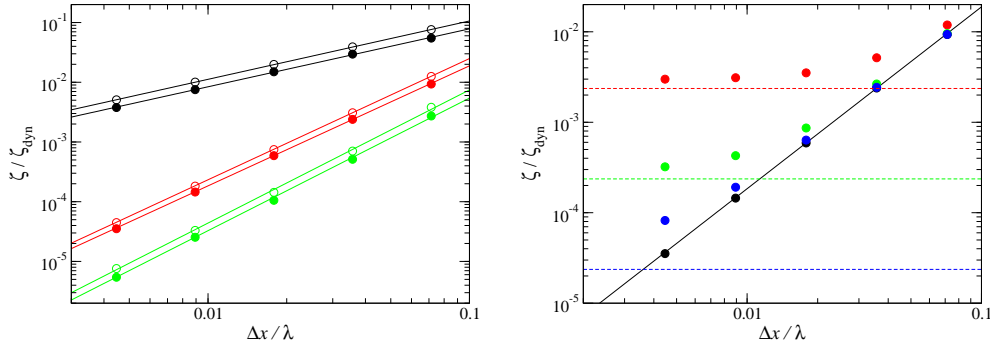


Figure 2. Dependence of the numerical viscosity ζ with the resolution in the case of the test sphere. The left panel shows the case without physical bulk viscosity for different flux formulae, Marquina (filled circles) and HLL (open circles), and different reconstruction schemes, constant (back), minmod (red) and MC (green). The right panel shows the case with Marquina flux formula and MC reconstruction for different values of the physical viscosity $\zeta = 10^{-4}$ (red) 10^{-5} (green), 10^{-6} (blue) and 0 (black). Dashed lines of the same color correspond to the value of the physical viscosity in each case.

using (B.9) it is possible to compute the physical bulk viscosity from the value of τ as

$$\zeta = \frac{\zeta_{\text{dyn}}}{\omega \tau}, \quad (9)$$

where $\zeta_{\text{dyn}} \equiv 2\rho_0 c_s^2 / \omega$ and c_s is the sound speed. The left panel of figure 2 shows the behavior of the numerical viscosity with the radial resolution for the different numerical schemes tested in simulations without physical bulk viscosity ($\zeta = 0$). To check the scaling with resolution we fit the viscosity values to a power law

$$\frac{\zeta}{\zeta_{\text{dyn}}} = S \left(\frac{\Delta x}{\lambda} \right)^p, \quad (10)$$

where $\lambda = 2\pi c_s \omega^{-1}$ is the wavelength of the oscillation mode, being c_s the speed of sound. The results of the fitted parameters S and p for the different numerical methods are shown in table 1. In all cases S is of order one, although in general the Marquina flux formula provides about 30% less bulk viscosity than the same simulation with HLL. The scaling does not change substantially with the flux formula but only with the reconstruction scheme: for constant reconstruction we recover first order convergence and for linear reconstruction (minmod and MC) second order. These fits allow us to compute the numerical bulk viscosity of different numerical schemes.

In the right panel of figure 2 we consider the simulations with physical bulk viscosity ($\zeta \neq 0$). In this case the viscosity of the code decreases with resolution with a similar scaling as in the case without physical viscosity. For sufficiently high resolution, the viscosity converges to the value of the added physical viscosity. Our method to estimate the bulk viscosity overestimates, in the convergent regime, the real physical viscosity by $\sim 25\%$. We have checked that the damping time and therefore the viscosity is not affected for a wide range of amplitudes of the perturbation (0.1 - 10^{-7}) and hence we can conclude that non-linear effects does not play any role in the damping observed during this test. We have also checked that the results are independent of the CFL factor used for the time-step, by changing its value between 0.8 and 10^{-3} . Since our final aim is to perform multidimensional simulations we have

Table 1. Coefficients S and p of the fitted numerical viscosity in radial oscillations of a test fluid sphere, for different flux formulae and reconstruction schemes.

Flux formula	reconstruc.	p	S
Marq.	constant	0.97	0.74
HLL	constant	0.98	1.06
Marq.	minmod	2.01	1.91
HLL	minmod	2.03	2.66
Marq.	MC	2.23	0.96
HLL	MC	2.23	1.28

also performed some axisymmetric 2D models of this spherical system. We have chosen two representative radial resolutions $n_r = 20$ and 80 and varied the angular resolution $n_\theta = 8, 16$ and 32 . In all cases the results are indistinguishable from the 1D spherical simulations with the same number of radial points.

4. Numerical damping of neutron stars

We apply our method to estimate viscosity in the case of radial oscillations of non-rotating neutron stars. Our initial model is a non-rotating relativistic equilibrium configuration (Tolman 1939, Oppenheimer & Volkoff 1939). We use a polytropic equation of state $P = K\rho^\Gamma$ with adiabatic index $\Gamma = 2$ and polytropic constant $K = 100$ (units of $G = c = M_\odot = 1$). We choose central rest mass density to be $\rho_c = 7.9 \times 10^{14} \text{ g cm}^{-3}$ and gravitational mass $M_g = 1.4M_\odot$. The resulting circumferential radius is $R_C = 14.16 \text{ km}$, and the isotropic radial coordinate at the surface of the star is $R = 12.0 \text{ km}$. We evolve the system in dynamic spacetime adding an initial perturbation of the radial velocity corresponding to the fundamental radial oscillation mode with an amplitude of 10^{-3} . To compute the eigenfunction of the fundamental mode necessary for the perturbation, we use the eigenfunction recycling technique described in Dimmelmeier *et al* 2006. We perform 1D spherical simulations with different radial resolutions of the fluid grid, $n_r = 80, 160, 320$ and 640 , which is equally spaced from the center to 14.4 km . The time-step is computed using the CFL condition for the eigenvalues of the hydrodynamics system, resulting in $\Delta t = 1.13 \times 10^{-3} \text{ ms}$ for a grid with $n_r = 80$ and a CFL factor 0.8. We use an artificial atmosphere to treat the vacuum surrounding the star as described in Dimmelmeier *et al* 2002. The treatment consists of resetting all numerical cells with ρ below a certain threshold to the value ρ_{atm} and setting the velocity to zero. The values for the threshold and the atmosphere are 10^{-6} and 10^{-10} times the initial central density respectively. We have checked that the results presented here do not change if we decrease the values of these two quantities. We use three radial domains for the spectral metric solver: two including the star and one compactified domain in the exterior. Each of the domains has either 17 or 33 collocation points for our low and high metric resolution simulations. Since the CFC approximation only contains elliptic equations, which are not restricted by the CFL condition, it is not necessary to solve the metric as frequently as the hydrodynamics equations. We use a metric computation rate of $n_r/8$, i.e. we compute the metric once every $n_r/8$ time step of the hydrodynamics. We use a parabolic extrapolation of all the metric quantities between consecutive metric computations, which has been shown to provide sufficient

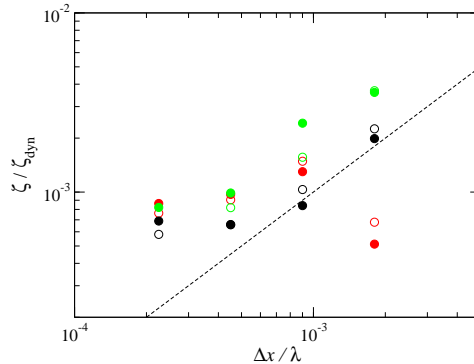


Figure 3. Dependence of the numerical viscosity ζ on the resolution in neutron star evolution. We show values for different flux formulae, Marquina (filled circles) and HLL (open circles), and different reconstruction schemes, constant (black), minmod (red) and MC (green). In all cases the highest metric resolution case is plotted. The dashed line represents the function $\zeta/\zeta_{\text{dyn}} = \Delta r/\lambda$.

accuracy during the evolution (Dimmelmeier *et al* 2002). We do not add physical bulk viscosity in any of the simulations ($\zeta = 0$), therefore the only dissipative processes in the evolution are of numerical nature. To compute the numerical bulk viscosity we use (9) as in the previous section but with $\zeta_{\text{dyn}} \equiv 2\bar{\rho}_0 c_s^2/\omega$ according to (B.14), where $\bar{\rho}$ is estimated as the central density. Since the numerical viscosity can depend on the location in the star the resulting value represents an average numerical viscosity. For our particular case and the fundamental radial mode ($\omega = 9.11 \times 10^3$ Hz) the resulting value is $\zeta_{\text{dyn}} = 3.99 \times 10^{31}$ g cm $^{-1}$ s $^{-1}$. This procedure gives us an idea of the order of magnitude of the averaged numerical viscosity on the star. More accurate computations of the damping-time could be done using the expressions of the appendix B or the procedure described in Cutler *et al* 1990.

Figure 3 shows the variation of the viscosity with the radial resolution normalized to the wavelength of the perturbation computed at the center of the star. In general the viscosity decreases with increasing resolution. However the lowest resolution case with the minmod reconstruction shows an anomalously low numerical viscosity, which we think is an artifact of the low resolution. We plot the function $\zeta/\zeta_{\text{dyn}} = \Delta r/\lambda$ for comparison. The general trend is roughly first order decreasing the order for the highest resolution models, although we are using both first and second reconstruction schemes. The reason for the lower order of convergence is that all reconstruction schemes reduce to first order at discontinuities. Since we encounter a discontinuity at the surface any evolution will inevitably lead to first order convergent results. This is also a strong indication that the main numerical dissipation process in the neutron star evolution is probably due to the surface of the star, and therefore increasing the reconstruction order does not decrease the mean numerical viscosity responsible for the damping of global oscillations.

We have checked the influence of the CFL factor, the metric calculation rate and the 2D effects for simulations with $n_r = 80$ radial points, Marquina flux formula and MC reconstruction. One of the main differences with respect to the spherical test case of the previous section is that the equations that we are solving have sources due to the gravity terms. In general the presence of non-zero sources can increase the stiffness of the problem leading to inaccurate solutions, even unstable for extremely stiff sources.

We expect some influence of the CFL factor in our simulations since the reduction of the time step tends to cure the stiffness problems. We have performed simulations with CFL factor 0.8 (standard for all previous simulations), 0.1, 0.01 and 0.001, with a metric computation rate of $10 \times 0.8 / (\text{CFL factor})$, which maintain constant the metric computation rate per unit evolution time. The amplitude of the oscillation at the end of the simulation varies about 0.5% at most. However most of the variation is observed between CFL factor 0.8 and 0.1, and decreasing the CFL factor further does not significantly changes the solution. Therefore the effect on the computed damping rate can be neglected. We find that the stiffness of the sources depends on how often the metric is computed. We also perform the same simulations with a metric computation rate 10. In this case the metric is computed more often per time unit than the previous one, as the CFL factor decreases. We find variations of about 25% in the final amplitude depending on the CFL factor used, although these variations depend strongly on the radial resolution. For $n_r = 160$ the maximum variation due to CFL factor changes is smaller than 10%. Since the effect of the CFL factor becomes larger lowering the metric computation rate, we can conclude that the sources become more stiff if the metric is computed more often. An explanation for this effect is that if the metric is computed less often, the sources vary due to the space-time evolution on time-scales longer, than the hydrodynamic variables, which reduces the stiffness. We conclude that the stiffness of the sources is not significantly affecting the computation of the damping rates for the metric computation rate that we use in our regular simulations. However special care should be taken in simulations in which the metric computation rate is high (close to one), e.g. in black hole formation simulations, since the stiffness of the sources could lead to an increasing of the numerical viscosity of the code if the CFL factor is not appropriately lowered. We also perform 2D-axisymmetric simulations with 4, 8 16 and 32 angular grid points. Since the initial perturbation is radial, non-radial modes are not excited. We find an error in the angular velocity which is of order $v^\theta/v^r \approx 10^{-9}$, and which is closely related to the accuracy of numerical recovery of the primitive variables. Since the angular extension of the grid restricts the time step of the simulation in a factor proportional to $1/n_\theta$, we find a similar behaviour increasing n_θ as it is found decreasing the CFL factor.

5. Discussion

We conclude that it is possible to estimate dissipation effects in numerical simulations which produce an effect similar to physical bulk viscosity. In a very simplified case, as the test fluid sphere of constant density, the numerical viscosity scales with the order of the reconstruction. In the application of our method to neutron stars simulations we find that the behaviour of the numerical viscosity is more complicated since the gravity sources also contribute to the numerical dissipation processes, and the presence of the surface lowers the scaling of the viscosity to first order.

To understand why the numerical inaccuracies can be modelled as a bulk viscosity term we consider the generic form of the flux formula in a Riemann solver

$$F_{\text{num}}^i = \bar{F}^i + \Lambda \Delta U, \quad (11)$$

where F_{num}^i is the numerical flux that is used in the time update, \bar{F}^i is an averaged value of the flux, ΔU represents the discontinuity at each cell interface and Λ the eigenvalue matrix. The particular form of the average and the matrix U depends on the particular Riemann solver. If a reconstruction scheme of order p is used, the value

of U at both sides of the interface in smooth regions of the flow agrees up to the $p - 1$ -th derivative, therefore for any function $f(U)$

$$\Delta f(U) \propto (\Delta r)^p \mathcal{D}^p U \quad (12)$$

where \mathcal{D}^p represents p -th spatial derivatives. If one applies this expression to the momentum equation

$$\partial_t (\sqrt{\gamma} S_j) + \partial_i \bar{F}^i + \mu (\Delta r)^p \mathcal{D}^{(p+1)} S_j = Q, \quad (13)$$

where μ depends on the specific Riemann solver used and Q represent the sources (r.h.s of (A.2)). The new term appearing in the numerical version of the equations is a dissipative term since it includes a $p+1$ derivative, while $\mu (\Delta r)^p$ is the corresponding dissipative coefficient. For first order reconstruction, the dissipation term includes second derivatives that resemble to a viscosity term with viscosity proportional to Δr . For higher order reconstruction the new term resembles hyperviscosity coefficients. Note that with this interpretation we can identify the computed value of ζ in our simulations with a viscosity or hyperviscosity term, which scales with resolution with the order of the reconstruction scheme. Furthermore, we can argue that, since the new terms in (13) are responsible for both the bulk viscosity and shear viscosity terms, the value of the numerical shear viscosity of the code has to be of the same order of magnitude as the numerical bulk viscosity estimated in this work. If this case were true, the method described in this paper could be a powerful tool to estimate numerical dissipative effects in multidimensional simulations. However the method has some limitations due to the approximations that we considered. The integral expressions (B.12) and (B.13) as well as the approximate expression for the expansion (4) rely on the facts that a post-Newtonian expansion is possible and that velocity perturbations are small. This provides an order-of-magnitude estimate in the case of systems involving neutron stars or proto-neutron stars since $\mathcal{O}(c^{-2}) \sim 0.15$. In this scenarios the velocity involved in oscillations is typically smaller than 0.1. In the vicinity of black holes, the post-Newtonian expansion is not convergent anymore, and the method can lead to large inaccuracies. Similar thing happens in the case of flows with a high Lorentz factor as those observed in jets.

From our simulations we also conclude that the gravity can be an important source of numerical viscosity which has to be estimated in an appropriate way. The stiffening of the sources in the presence of rapidly changing spacetime, can lead to a strong increasing in the numerical viscosity if the CFL condition is not adapted accordingly. Although this effect is not a problem in the simulations presented in this work, it could be in case in which the spacetime evolves in similar time-scales as the fluid, e.g. in the formation of a black hole. It is therefore important to test in the future which are the real effects of numerical viscosity in such simulations.

Finally, we note that all the viscosity results given in this paper are normalized to ζ_{dyn} , which depends on the frequency of the oscillation ω . For a given astrophysical scenario, and the same numerical resolution, different modes will be affected in a different way depending on the frequency of the mode. Therefore, in order to estimate the resolution needed to evolve a system for a given amount of time with reasonably small damping one has to use the mode with higher frequency, of those who may be important in the dynamics of the system. Deciding which is this mode may be non trivial in non-linear simulations, since a strong numerical damping in high frequency modes, which are coupled to the lower frequency modes, can modify the damping times for the low frequency modes too.

Acknowledgments

This work was supported by the Collaborative Research Center on Gravitational Wave Astronomy of the Deutsche Forschungsgesellschaft (DFG SFB/Transregio 7). I would like to thank Ewald Müller for his comments on the paper and Klaus Dolag for some useful discussions about viscosity.

Appendix A. Radial oscillations of an homogeneous sphere.

We consider a spherically symmetric barotropic fluid in Minkowski spacetime, with equation of state $P = P(\rho)$. The hydrodynamics equations (A.1) and (A.2) in this case read:

$$\partial_t (\rho W) + \frac{1}{r^2} \partial_r [r^2 \rho W v] = 0, \quad (\text{A.1})$$

$$\partial_t (\rho \hat{h} W^2 v) + \frac{1}{r^2} \partial_r [r^2 \rho \hat{h} W^2 v^2] = -\partial_r \hat{P}, \quad (\text{A.2})$$

where $v \equiv v^r$. The equilibrium solution of this system is trivially zero velocity, $v_0 = 0$, and constant pressure, $P = P_0$, and hence constant rest mass density, $\rho = \rho_0$. We consider perturbations of the rest mass density and velocity, $\rho = \rho_0 + \rho'$ and $v = v'$, and hence

$$P = P_0 + \frac{\partial P_0}{\partial \rho_0} \rho' = P_0 + h_0 c_s^2 \rho'. \quad (\text{A.3})$$

where c_s^2 is the speed of sound of the equilibrium model. The linearized hydrodynamics equations read

$$\partial_t v' + \frac{c_s^2}{\rho_0} \partial_r \rho' - \frac{\zeta}{\rho_0 h_0} \partial_r \Theta = 0, \quad (\text{A.4})$$

$$\partial_t \rho' + \rho_0 \partial_r v' + \frac{2}{r} \rho_0 v' = 0, \quad (\text{A.5})$$

If ζ is sufficiently small, i.e. $\zeta \ll h_0 \rho_0$, the viscosity terms can be neglected in the computation of the perturbations spectrum. In this case equations (A.4) and (A.5) can be combined in a wave equation for ρ'

$$\partial_{tt} \rho' - c_s^2 \partial_{rr} \rho' - \frac{2c_s^2}{r} \partial_r \rho' = 0. \quad (\text{A.6})$$

The system of equations (A.4) and (A.5) admits oscillatory solutions of the form $v' = A(r) \sin \omega t$ and $\rho' = B(r) \cos \omega t$ and hence (A.6) results in

$$\partial_{rr} B + \frac{2}{r} \partial_r B + \frac{\omega^2}{c_s^2} B = 0. \quad (\text{A.7})$$

This equation has the form of the Lane-Emden equation of index 1, which have solutions regular at $r = 0$ (Chandrasekhar 1967) of the form

$$B(r) = \rho'_0 \frac{\sin(kr)}{kr}, \quad (\text{A.8})$$

where $k = \omega/c_s$ and ρ'_0 is a parameter which controls the amplitude of the density perturbation. From (A.4) the solution for the velocity perturbation is

$$A(r) = v'_0 \frac{kr \cos(kr) - \sin(kr)}{(kr)^2}, \quad (\text{A.9})$$

where v'_0 controls the amplitude of the velocity perturbation and is related to ρ'_0 by

$$\frac{\rho'_0}{\rho_0} = -\frac{v'_0}{c_s}. \quad (\text{A.10})$$

If we impose boundary conditions at the surface $v'(R) = 0$, i.e., $A(R) = 0$ we find a discrete spectrum of modes given by the solutions of

$$\tan(kR) = kR. \quad (\text{A.11})$$

We have computed the roots of this equations by means of a bisection algorithm. The first five numerical solutions correspond to $kR = 4.49, 7.73, 10.90, 14.07$ and 17.11 .

Appendix B. Damping time of an oscillating spherical star

The rate of change of the energy due to bulk viscosity of a pulsating star is (cf. Cutler *et al* 1990)

$$\frac{dE}{dt} = -4\pi \int_0^R dr r^2 \phi^6 \zeta |\Theta|^2, \quad (\text{B.1})$$

and, provided that the energy of the pulsations E is known, the damping time is

$$\tau = -2E \left\langle \frac{dE}{dt} \right\rangle^{-1}. \quad (\text{B.2})$$

where $\langle \rangle$ denotes the time average over a cycle.

The energy stored in the radial oscillations of a spherical star can be computed as the energy difference between the star in equilibrium and the perturbed system. Previous computations (Meltzer & Thorne 1966, Glass & Lindblom 1983) used Schwarzschild coordinates in their computations. Instead of performing the coordinate transformation to the choice of the present work we find it easier and more instructive to compute the energy of the oscillations directly in our coordinates, although the result should be identical.

The ADM energy is a conserved quantity which in spherical symmetry and under our gauge choice is

$$E_{\text{ADM}} = -2 \int_0^R dr r^2 \Delta \phi = 4\pi \int_0^R dr r^2 \phi^5 \left(\rho h W^2 - P + \frac{K_{ij} K^{ij}}{16\pi} \right), \quad (\text{B.3})$$

being Δ the Laplacian with respect to the flat 3-metric and K_{ij} the extrinsic curvature of the induced 3-metric γ_{ij} . Since the extrinsic curvature vanishes for the equilibrium system in our gauge choice the equilibrium ADM energy is

$$E_{\text{ADM}0} = 4\pi \int_0^R dr r^2 \phi_0^5 (\rho_0 h_0 - P_0). \quad (\text{B.4})$$

The ADM energy does not change with time and hence we can compute its value by evaluating the integral at the oscillation phase with maximum velocity. In this phase, due to the continuity equation (A.1), the variation of $\phi^6 \rho W$ with respect to the equilibrium is zero. The leading term in the perturbation corresponds to quadratic terms in the velocity. The energy of the oscillations is thus $E = E_{\text{ADM}} - E_{\text{ADM}0}$ which results in

$$E = 4\pi \int_0^R dr r^2 \phi_0^5 \left[\rho_0 h_0 \frac{1}{2} v'^2 - (\rho_0 h_0 - 5P_0) \frac{\phi'}{\phi} + \frac{K'_{ij} K'^{ij}}{16\pi} \right] \quad (\text{B.5})$$

for adiabatic perturbations. Note that here $\phi' = \phi - \phi_0$ corresponds to the variation of ϕ with respect to the equilibrium for the phase in which v' is maximum and hence is a term quadratic in v' .

If we apply this expressions to the case of the spherical fluid in Minkowski spacetime of the appendix A the resulting expressions are

$$E = 4\pi \int_0^R dr r^2 \frac{1}{2} \rho_0 A(r)^2 = \rho_0 v_0'^2 \pi \frac{R}{k^2} \sin^2(kR), \quad (\text{B.6})$$

$$\left\langle \frac{dE}{dt} \right\rangle = -\zeta v_0'^2 \pi R \sin^2(kR), \quad (\text{B.7})$$

where we have explicitly used that (A.11) is fulfilled to perform the integration and that $\langle |\Theta|^2 \rangle = \langle (\nabla A)^2 \rangle / 2 = \omega^2 B^2 / (2\rho_0^2)$. The damping time is therefore

$$\tau = \frac{2\rho_0 c_s^2}{\zeta \omega^2}, \quad (\text{B.8})$$

It is convenient to express it as

$$\omega\tau = \frac{\zeta_{\text{dyn}}}{\zeta} \quad (\text{B.9})$$

where $\zeta_{\text{dyn}} \equiv 2\rho_0 c_s^2 / \omega$. For $\zeta \sim \zeta_{\text{dyn}}$ the damping of the mode occurs in dynamical time-scales, while if $\zeta \ll \zeta_{\text{dyn}}$ the damping occurs in secular timescales.

In the case of a perturbed relativistic star the computation of the damping rate can not be computed analytically. However we can still make an order of magnitude estimation. For this purpose it is useful to truncate the equations (B.1) and (B.5) to the leading order in the post-Newtonian expansion

$$E = 4\pi \int_0^R dr r^2 \frac{1}{2} \rho_0 v'^2 (1 + \mathcal{O}(c^{-2})), \quad (\text{B.10})$$

$$\frac{dE}{dt} = -4\pi \int_0^R dr r^2 \zeta |\Theta|^2 (1 + \mathcal{O}(c^{-2})). \quad (\text{B.11})$$

which corresponds to the Newtonian expression for the kinetic energy, being $\mathcal{O}(c^{-2}) \sim \mathcal{O}(v^2) \sim \mathcal{O}(GM/R)$ the first post-Newtonian corrections (see e.g. Blanchet *et al* 1980). If we assume $e^{i(\omega t + kr)}$ dependence of the perturbations, where k is the wavenumber, then $\langle |\Theta|^2 \rangle \sim k^2 \langle v^2 \rangle = k^2 v_{\text{max}}^2 / 2$. The energy and energy losses result in this case

$$E = 2\pi \int_0^R dr r^2 \rho_0 v_{\text{max}}^2 (1 + \mathcal{O}(c^{-2})), \quad (\text{B.12})$$

$$\left\langle \frac{dE}{dt} \right\rangle \sim -2\pi k^2 \zeta \int_0^R dr r^2 v_{\text{max}}^2 (1 + \mathcal{O}(c^{-2})), \quad (\text{B.13})$$

and hence

$$\omega\tau \sim \frac{2\omega \bar{\rho}_0}{k^2 \zeta} = \frac{2\bar{\rho}_0 c_s^2}{\zeta \omega} = \frac{\zeta_{\text{dyn}}}{\zeta}, \quad (\text{B.14})$$

where $\bar{\rho}$ is an averaged density weighed by the eigenfunction $A(r)$ and $\zeta_{\text{dyn}} \equiv 2\bar{\rho}_0 c_s^2 / \omega$.

References

- Anninos P, Fragile P C and Salmonson J D 2005 *Astrophys. J.* **635** 723
- Antón L *et al* 2006 *A&A* **637** 296
- Baiotti L *et al* 2005 *Phys Rev D* **71** 024035
- Cerdá-Durán P, Font J A, Antón L and Müller E 2007 *Astron. Astrophys.* **492** 937
- Cerdá-Durán P, Font J A and Dimmelmeier H 2007 *Astron. Astrophys.* **474** 169
- Chandrasekhar S 1967 *An introduction to the Study of Stellar Structure* New York:Dover p 84
- Cutler C, Lee L and Splinter R J 1990 *Astrophys. J.* **363** 603
- Courant R, Friedrichs K and Lewy H 1928 *Math. Ann.* **100** 32
- Courant R, Friedrichs K and Lewy H 1967 *IBM J. Res. Dev.* **11** 215 (English translation of Courant *et al* 1928)
- Cordero-Carrión *et al* 2009 *Phys. Rev. D* **79** 24017
- Dimmelmeier H, Font J A and Müller E 2002 *Astron. Astrophys.* **388** 917
- Dimmelmeier H, Novak J, Font J A, Ibáñez J M and Müller E 2005 *Phys. Rev. D* **71** 064023
- Dimmelmeier H, Stergioulas N and Font J A 2006 *Mon. Not. R. Astron. Soc.* **368** 1609-1630
- Duez M, Marronetti P, Shapiro S L and Baumgarte T W 2003 *Phys. Rev. D.* **67** 024004
- Donat R, Font J A, Ibáñez J M and Marquina A 1998 *J. Comput. Phys.* **146** 58
- Fragile P C, Lindner C C, Anninos P and Salmonson J D 2009 *Astrophys. J.* **691** 482
- Fromang S and Papaloizou J 2007 *Astron. Astrophys.* **476** 1113
- Gammie C F, McKinney J C and Toth G 2003 *Astrophys. J.* **589** 444
- Glass E N and Lindblom L 1983 *Astrophys. J. S.* **53** 93
- Harten A, Lax P D and van Leer B 1983 *SIAM Rev.* **25** 35
- Herring J R, Orszag S A, Kraichnan R H and Fox D G 1974 *J. Fluid Mech.* **66** 417
- Ibáñez J M, Aloy M A, Font J A, Martí J M, Miralles J A and Pons J A 2000 *Proc. Conf. on Godunov methods: theory and applications (Oxford)* ed E F Toro (Kluwer Academic/Plenum Publishers) p 485-496
- Isenberg J A 2008 *Int. J. Mod. Phys. D* **17** 265
- Komissarov S S 2005 *Mon Not R Astron Soc* **359** 801
- Landau L D and Lifshitz E M 1987 *Fluid mechanics* (Amsterdam: Elsevier) p 44
- Marek A and Janka H T 2009 *Astrophys. J.* **694** 664
- MacFadyen A I, Woosley S E and Heger A 2001 *Astrophys. J.* **550** 410
- Meltzer D W and Thorne K S 1966 *Astrophys. J.* **145** 514
- Modjaz M *et al* 2008 *Astrophys. J.* **135** 1136
- Müller E and Janka H T 1997 *Astrophys. J.* **317** 140
- Porter D H and Woodward H P 1994 *Astrophys. J. S.* **93** 309
- Simon J B and Hawley J F 2009 *Astrophys. J.* **707** 883
- Simon J B, Hawley J F and Beckwith K 2009 *Astrophys. J.* **690** 974
- Tolman R C 1939 *Phys. Rev.* **55** 364
- Oppenheimer J R and Volkoff G M 1939 *Phys. Rev.* **55** 374
- Shibata M 2003 *Phys Rev D* **67** 024033
- Tompson C and Duncan R C 1993 *Astrophys. J.* **408** 194
- Wilson J R, Mathews, G J and Marronetti P 1996 *Phys. Rev. D* **54** 1317
- Woosley S E 1993 *Astrophys. J.* **405** 273
- Zink B, Schnetter E and Tiglio M 2008 *Phys Rev. D* **77** 103015